SUPPLEMENTARY INFORMATION

Design and synthesis of Janus-structured mutually-doped SnO_2-Co_3O_4 hollow nanostructures as superior anode materials for lithium-ion batteries

Gi Dae Park[a], Jung-Kul Lee*[b] and Yun Chan Kang*[a]

[a]Department of Materials Science and Engineering, Korea University, Anam-dong, Seongbuk-gu, Seoul 136-713, Republic of Korea

E-mail: yckang@korea.ac.kr Fax: +82-2-928-3584

[b]Department of Chemical Engineering, Konkuk University, Hwayang-dong, Gwangjin-gu Seoul 143-701, Republic of Korea, E-mail: jkrhee@konkuk.ac.kr

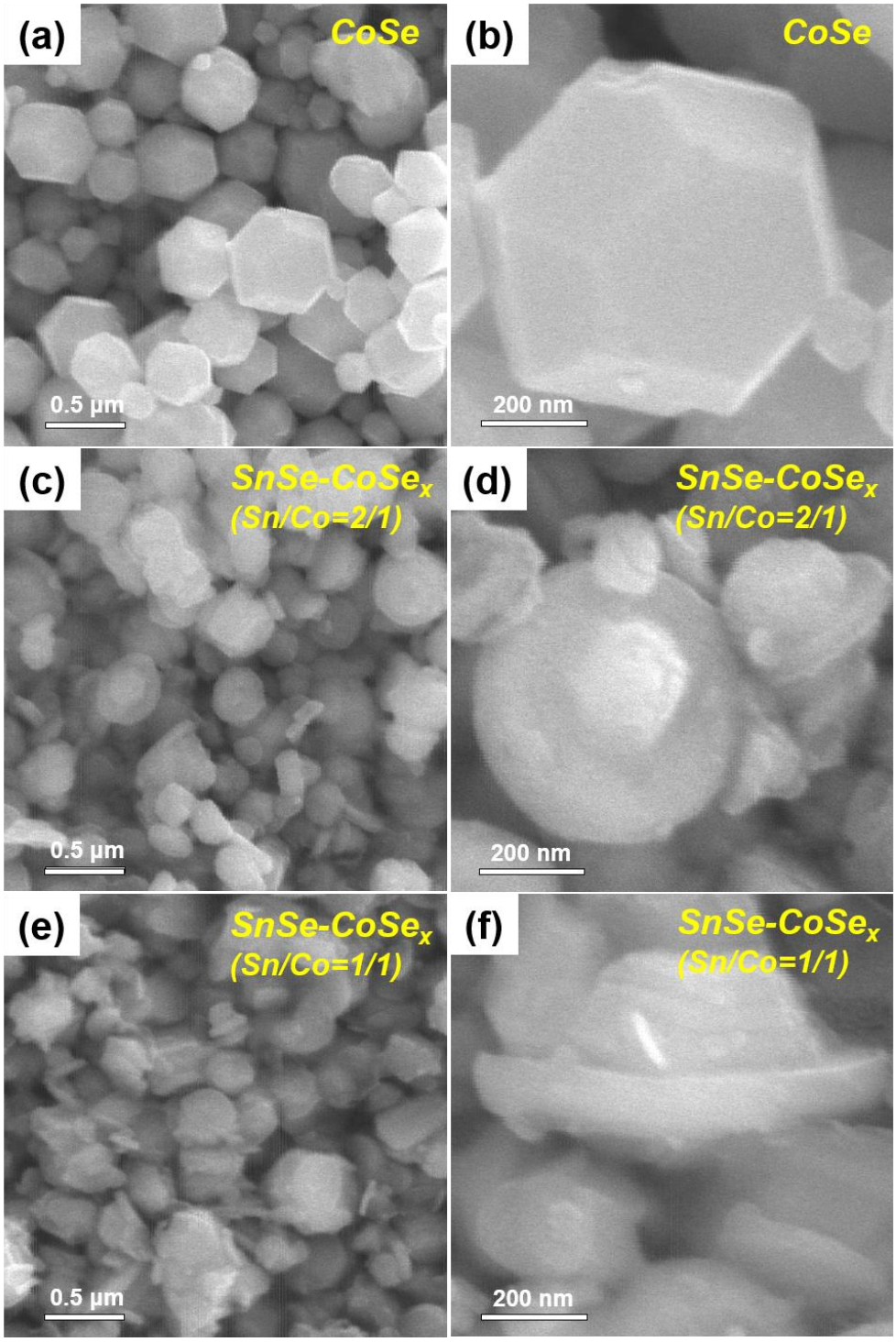

Fig. S1 Morphologies of the $CoSe_2$ and Janus-structured mutually-doped SnSe-$CoSe_x$ powders doped with each other material prepared by one-pot spray pyrolysis: (a,b) CoSe, (c,d) Sn/Co = 2/1, and (e,f) Sn/Co = 1/1.

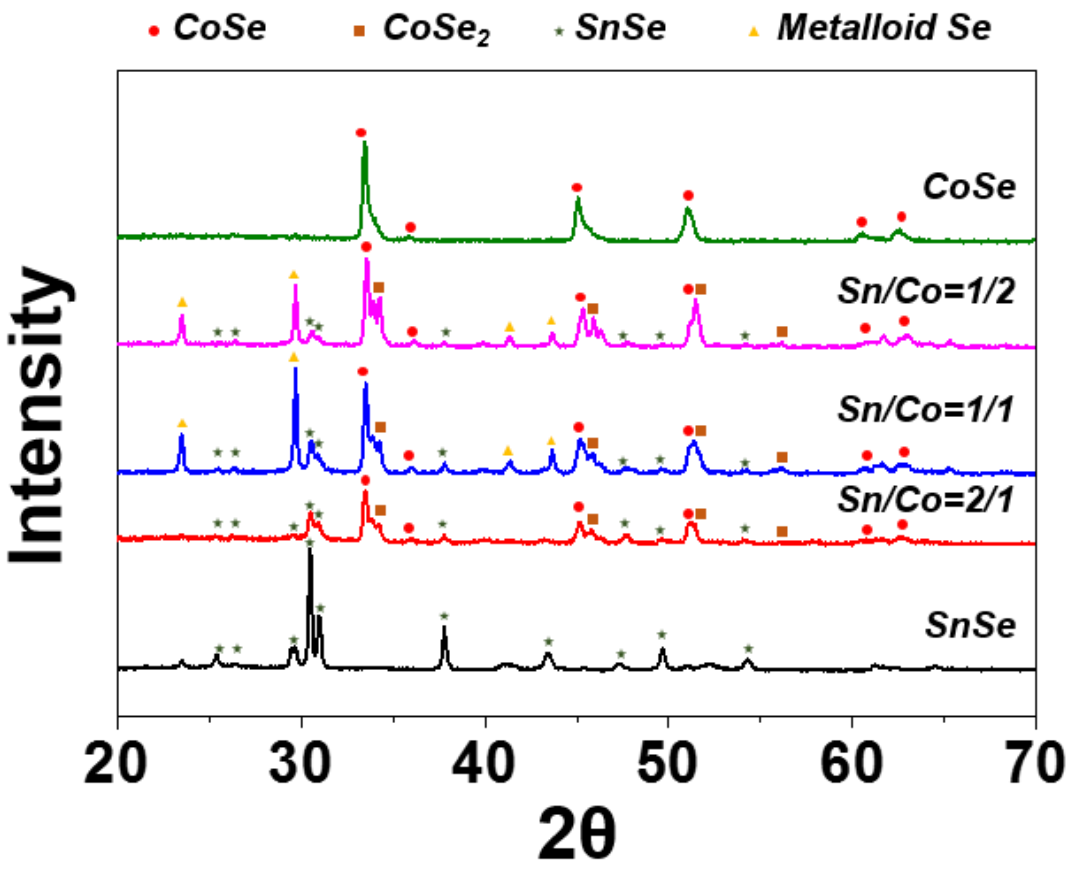

Fig. S2 XRD patterns of the SnSe, $CoSe_x$ and Janus-structured mutually-doped SnSe-$CoSe_x$ powders prepared by one-pot spray pyrolysis.

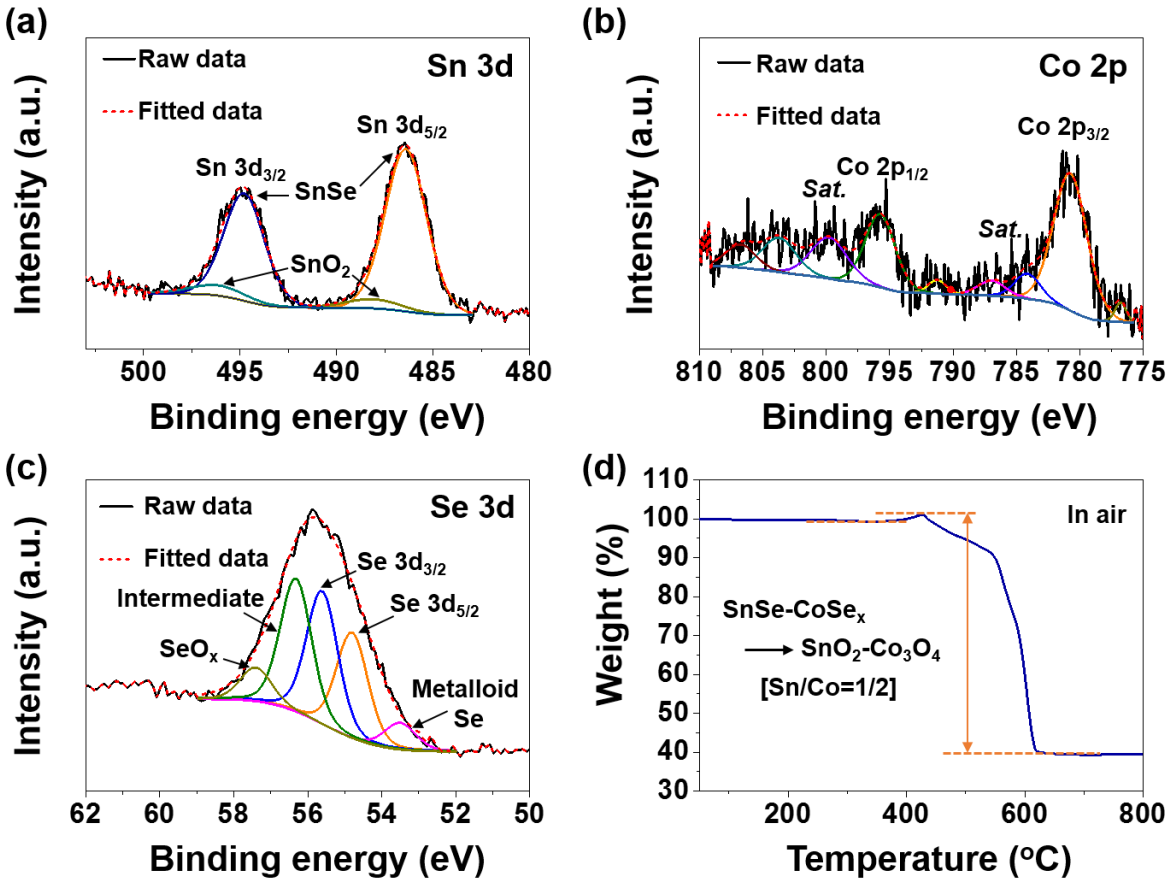

Fig. S3 (a-c) XPS spectra and (d) TG curve of the Janus-structured mutually-doped SnSe-$CoSe_x$ powders with Sn/Co ratio of 1/2 formed by one-pot spray pyrolysis: (a) Sn, (b) Co, (c) Se, and (d) TG curve.

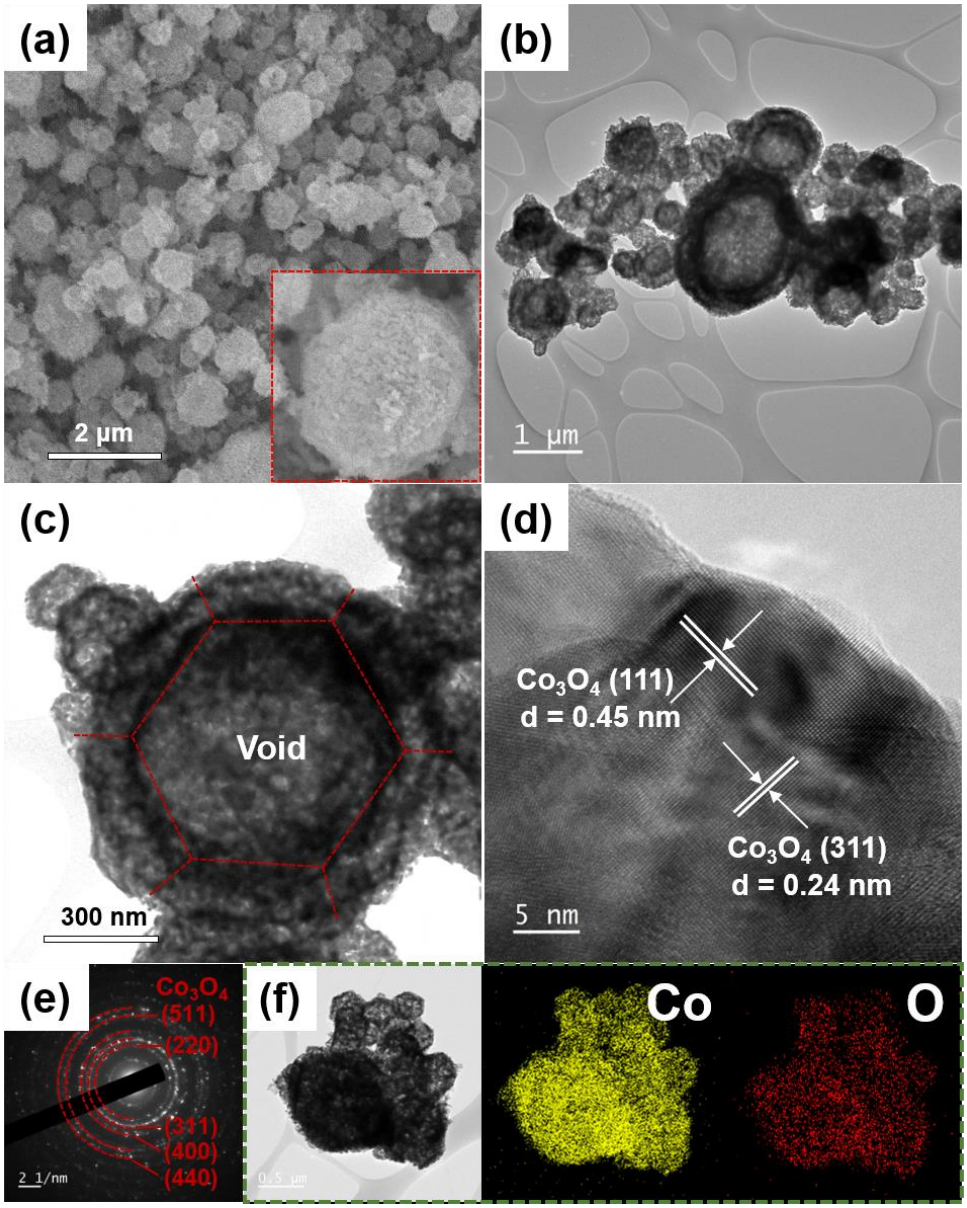

Fig. S4 Morphologies of the Co_3O_4 hollow polyhedron formed by nanoscale Kirkendall diffusion process: (a) SEM, (b,c) TEM, (d) high-resolution TEM images, (e) SAED pattern, and (f) elemental mapping images.

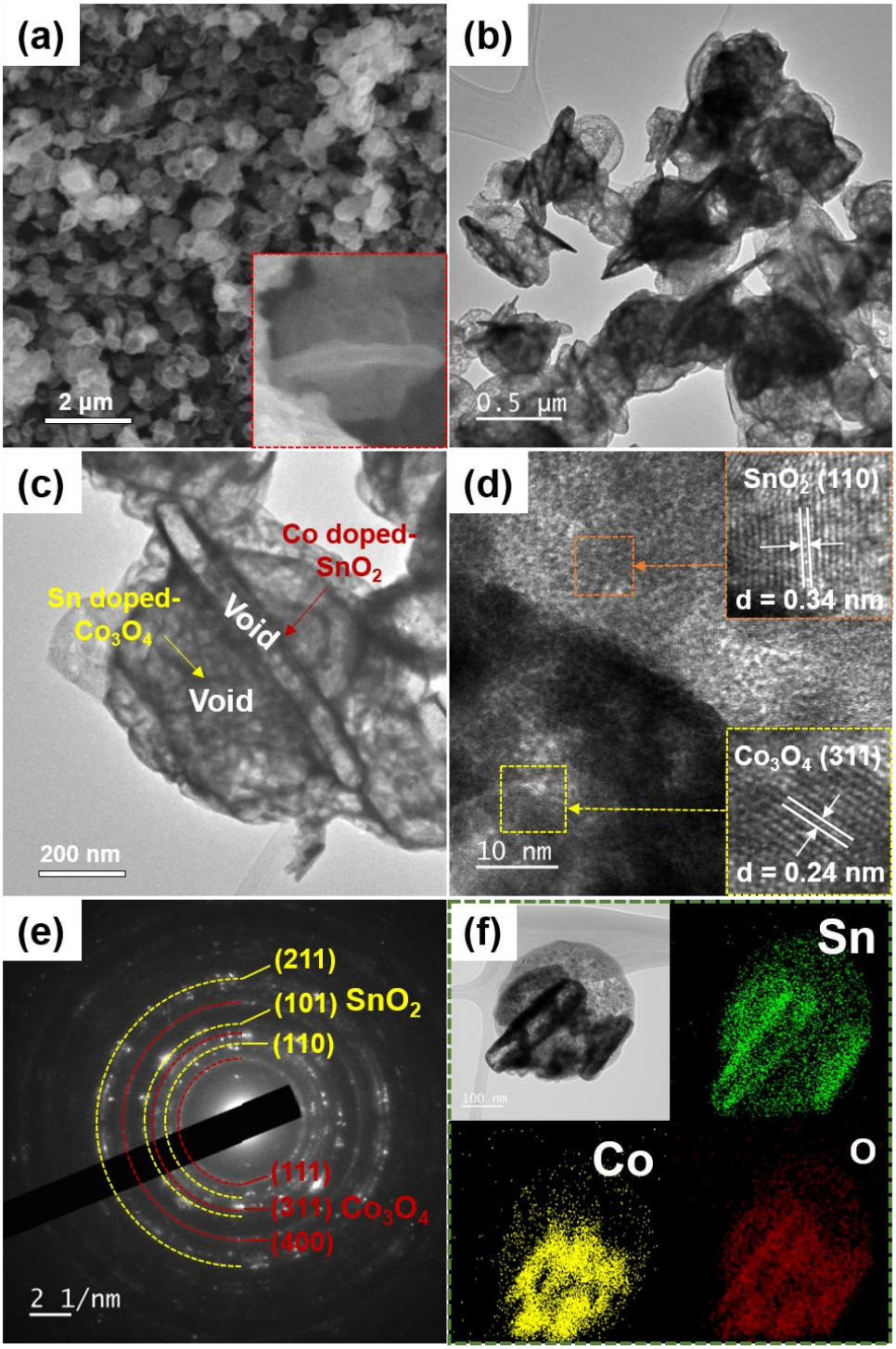

Fig. S5 Morphologies of the Janus-structured mutually-doped SnO_2-Co_3O_4 powders with Sn/Co ratio of 1/1 formed by nanoscale Kirkendall diffusion process: (a) SEM, (b,c) TEM, (d) high-resolution TEM images, (e) SAED pattern, and (f) elemental mapping images.

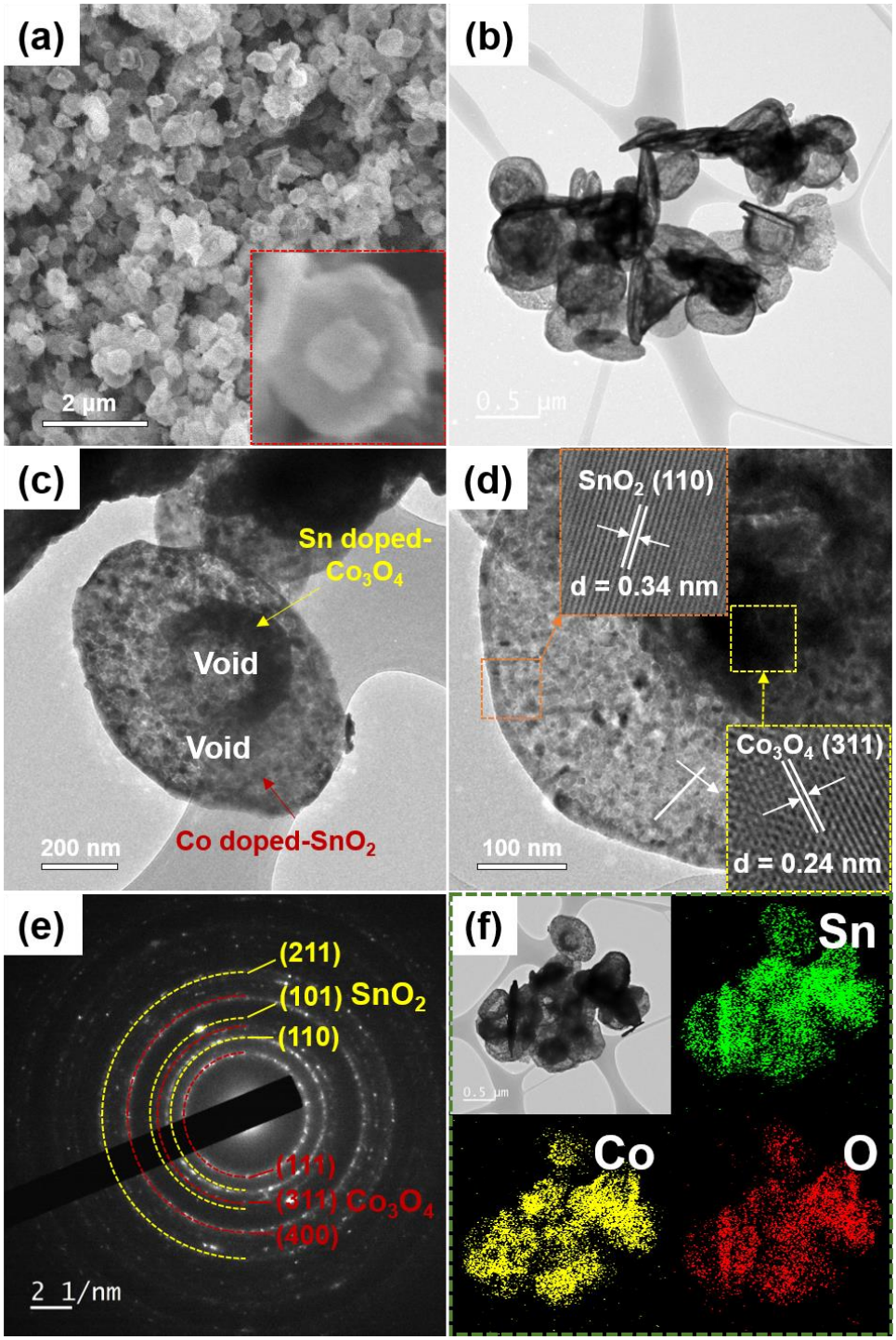

Fig. S6 Morphologies of the Janus-structured mutually-doped SnO_2-Co_3O_4 powders with Sn/Co ratio of 2/1 formed by nanoscale Kirkendall diffusion process: (a) SEM, (b,c) TEM, (d) high-resolution TEM images, (e) SAED pattern, and (f) elemental mapping images.

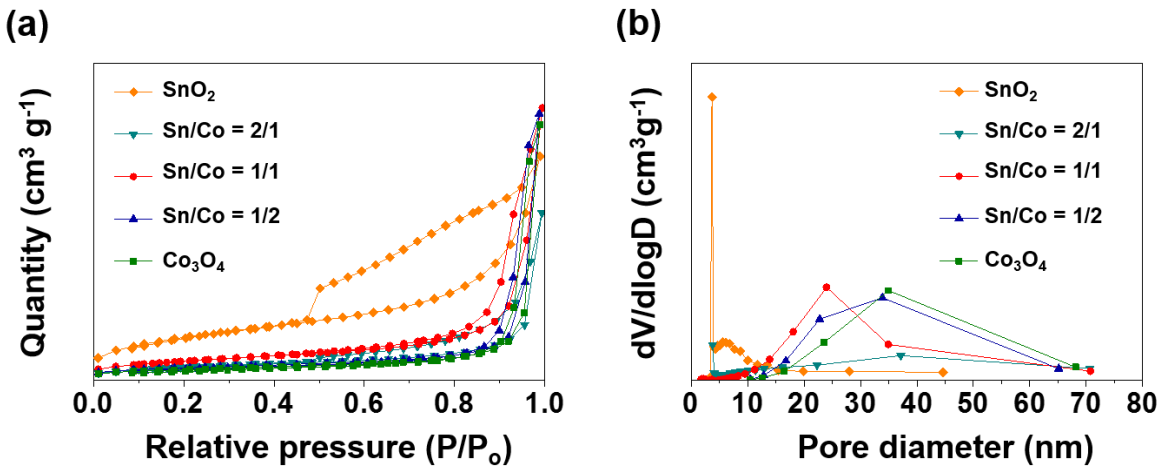

Fig. S7 N_2 adsorption and desorption isotherms and BJH pore size distributions of the SnO_2, Co_3O_4, and Janus-structured mutually-doped SnO_2-Co_3O_4 powders formed by nanoscale Kirkendall diffusion process.

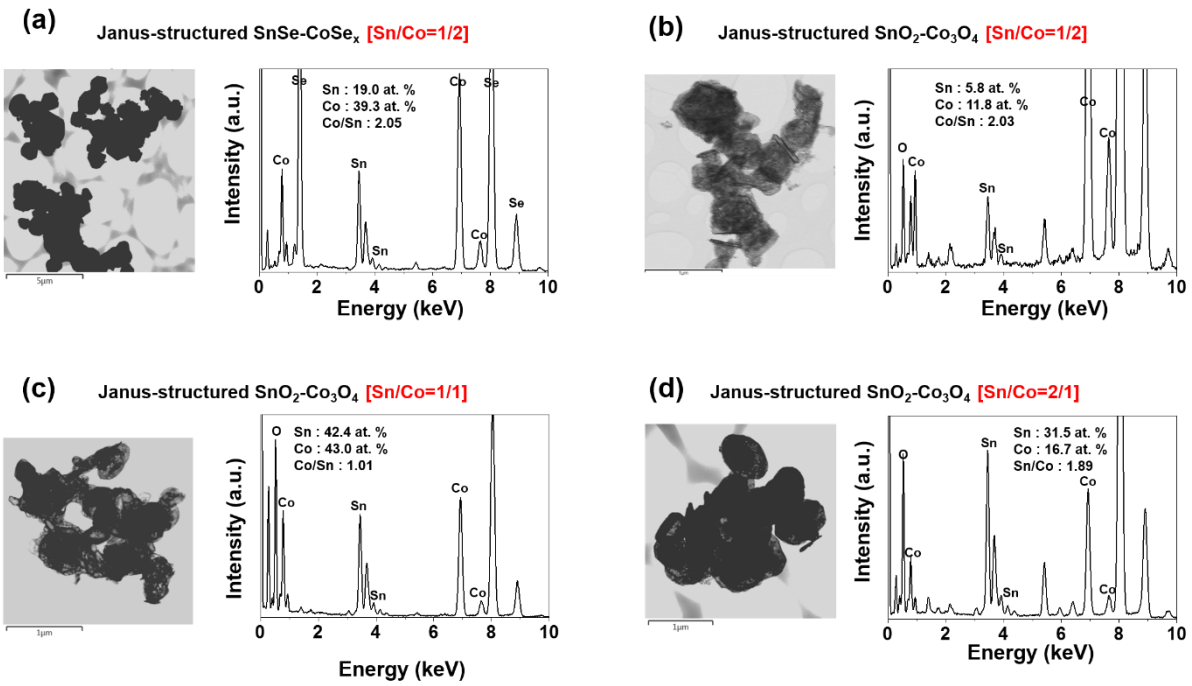

Fig. S8 EDS data of Janus-structured SnSe-$CoSe_x$ (Sn/Co=1/2) and SnO_2-Co_3O_4 (Sn/Co=1/2,1/1, 2/1) powders.

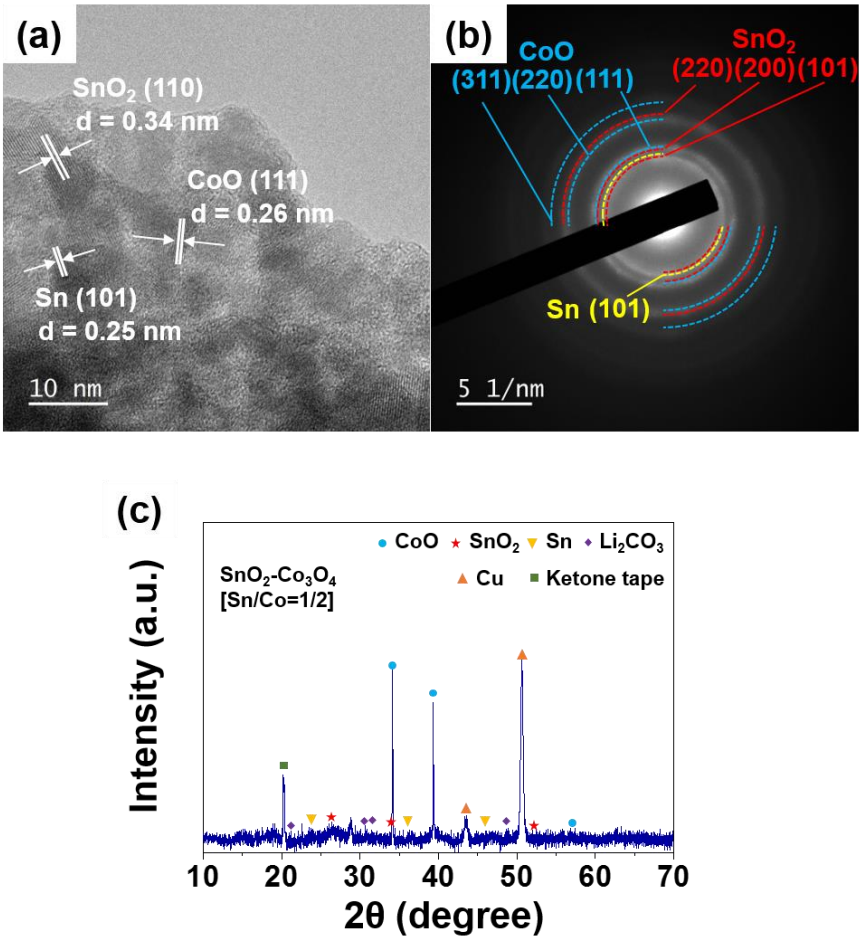

Fig. S9 Characteristics of Janus-structured SnO_2-Co_3O_4 powders (Sn/Co=1/2) obtained after 50th charge process at a current density of 1 A g^{-1}: (a) high resolution TEM image, (b) SAED pattern, and (c) XRD pattern.

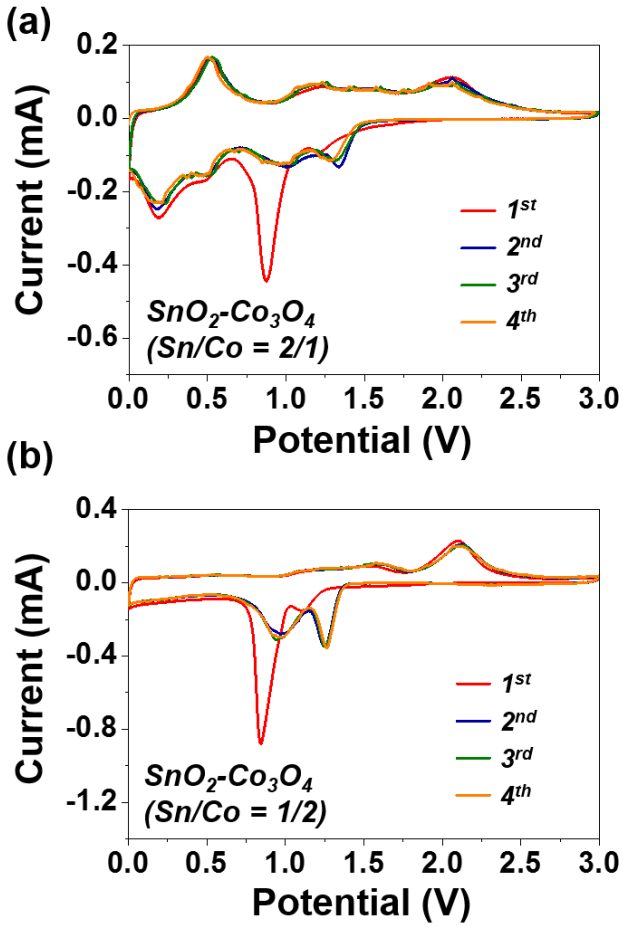

Fig. S10 CV curves of the Janus-structured mutually-doped SnO_2-Co_3O_4 powders formed by nanoscale Kirkendall diffusion process: (a) SnO_2-Co_3O_4 (Sn/Co = 2/1), (b) SnO_2-Co_3O_4 (Sn/Co = 1/2).

.

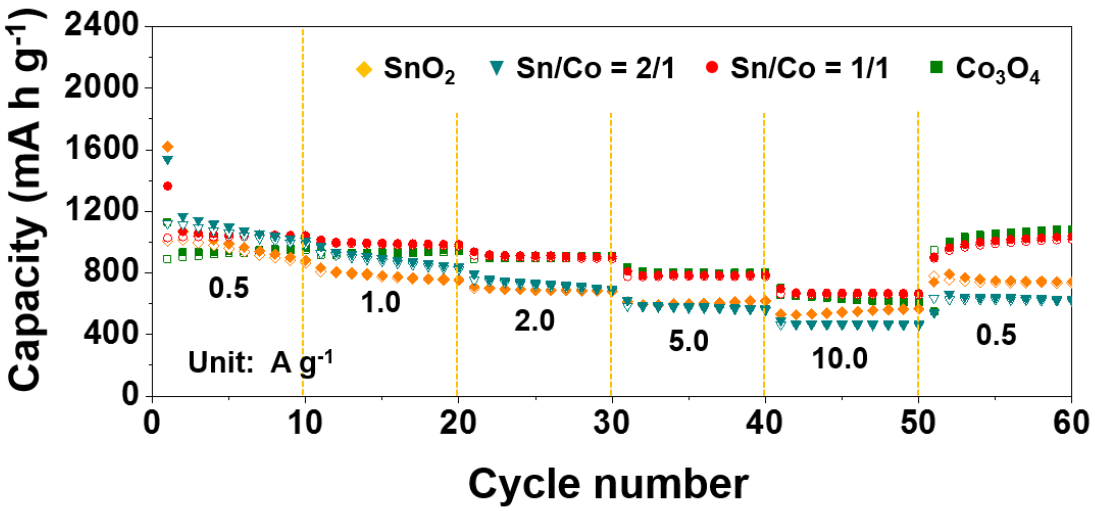

Fig. S11 Rate performances of the SnO_2, Co_3O_4, and Janus-structured mutually-doped SnO_2-Co_3O_4 powders formed by nanoscale Kirkendall diffusion process.

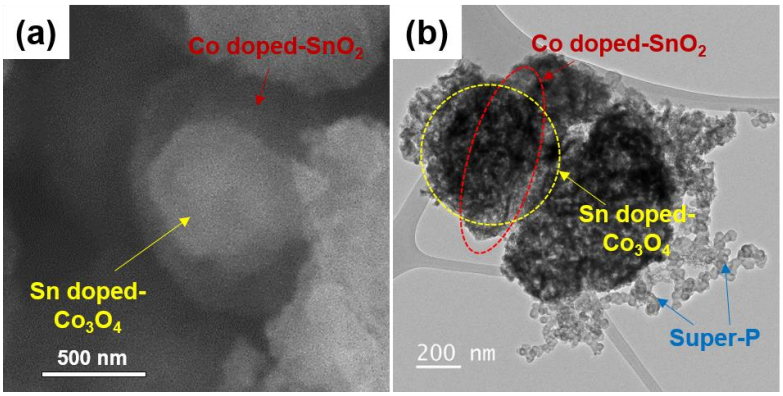

Fig. S12 Morphologies of Janus-structured SnO_2-Co_3O_4 powders (Sn/Co=1/2) obtained after 50 cycles at a current density of 1 A g^{-1}: (a) SEM, (b) TEM images.

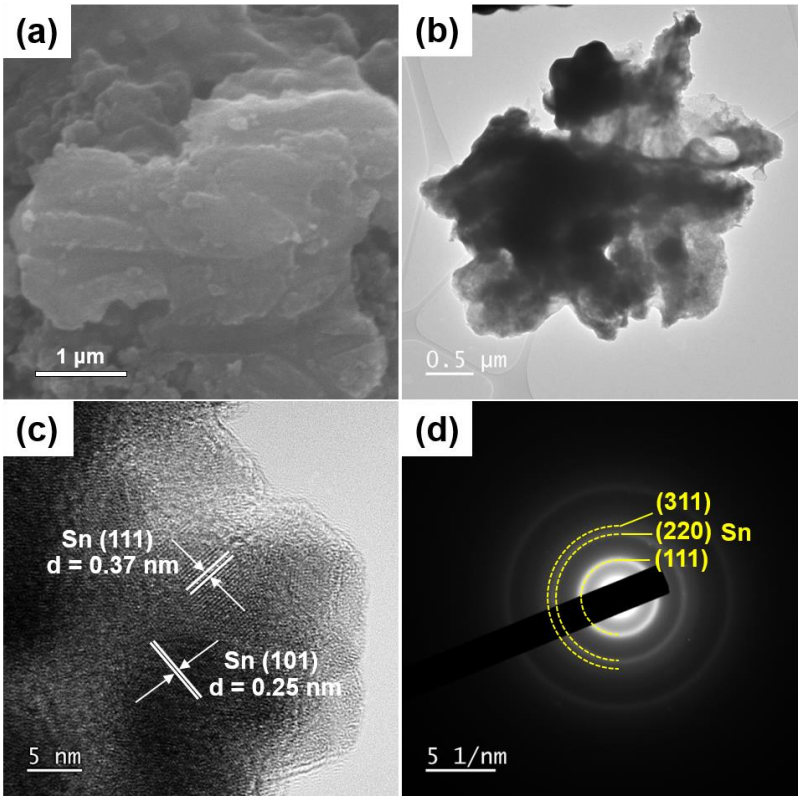

Fig. S13 Morphologies of bare SnO_2 nanoplates obtained after 50 cycles at a current density of 1 A g^{-1}: (a) SEM, (b) TEM image, (c) high resolution TEM image, and (d) SAED pattern.

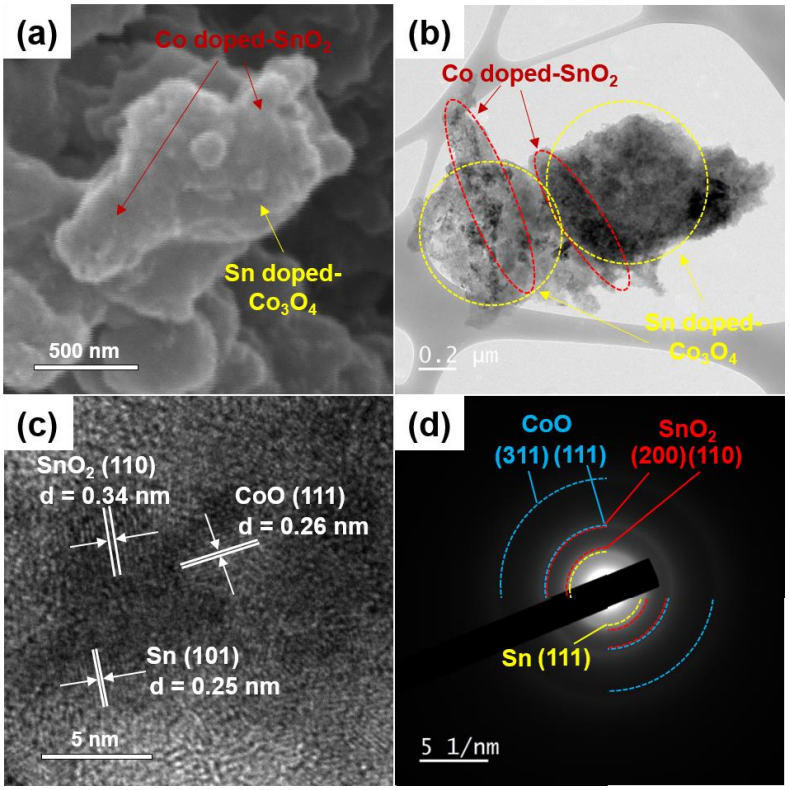

Fig. S14 Morphologies of Janus-structured SnO_2-Co_3O_4 powders (Sn/Co=1/2) obtained after 1000 cycles at a current density of 1 A g^{-1}: (a) SEM, (b) TEM image, (c) high resolution TEM image, and (d) SAED pattern.

Table S1. Electrochemical properties of various nanostructured SnO_2, Co_3O_4 and SnO_2-Co_3O_4 materials applied as lithium-ion batteries reported in the previous literatures.

Materials	Voltage range (V)	Current rate	Discharge capacity [mA h g^{-1}] and (cycle number)	Rate capacity [mA h g^{-1}] (current rate)	Ref
Interconnected SnO_2 nanoparticles	0.01-1.5	0.39 A g^{-1}	564 (100)	290 (4.7 A g^{-1})	[1]
SnO_2 hollow nanoplates	0.001-3.0	1.0 A g^{-1}	635 (300)	267 (30.0 A g^{-1})	[2]
Hierarchically structured SnO_2 microspheres	0.001-3.0	1.0 A g^{-1}	538 (300)	158 (30.0 A g^{-1})	[3]
Amorphous SnO_2 nanomembrane	0.003-3.0	1.6 A g^{-1}	854 (1000)	149 (40.0 A g^{-1})	[4]
Mesoporous SnO_2 nanowire	0-1.2	0.4 A g^{-1}	773 (50)	250 (20.0 A g^{-1})	[5]
Hierarchical SnO_2 hollow nanostructures	0.05-2.0	0.1 A g^{-1}	540 (50)	460 (7.8 A g^{-1})	[6]
SnO_2 hollow nanospheres	0.001-1.0	2.0 A g^{-1}	643 (300)	597 (7.0 A g^{-1})	[7]
Porous structured SnO_2	0.01-3.0	0.1 A g^{-1}	645 (50)	370 (5.0 A g^{-1})	[8]
Mesoporous Co_3O_4 nanowire arrays	0.01-3.0	0.078 A g^{-1}	700 (20)	450 (15.6 A g^{-1})	[9]
Co_3O_4 nanosheet-assembled multishelled hollow spheres	0.01-3.0	0.45 A g^{-1}	866 (50)	500 (1.78 A g^{-1})	[10]
Hollow-structured Co_3O_4 nanoparticles	0.05-3.0	0.45 A g^{-1}	880 (50)	450 (2.0 A g^{-1})	[11]
Micro-/nanostructured Co_3O_4 cubes	0.01-3.0	0.89 A g^{-1}	980 (60)	130 (8.9 A g^{-1})	[12]
Mesoporous Co_3O_4 nanoflakes	0.01-3.0	0.89 A g^{-1}	883 (300)	285 (8.9 A g^{-1})	[13]
Mesoporous single-crystalline Co_3O_4 nanobelts	0-3.0	1.0 A g^{-1}	980 (60)	605 (3.0 A g^{-1})	[14]
Co_3O_4 nanocages	0.05-3.0	0.05 A g^{-1}	854 (30)	252 (2.0 A g^{-1})	[15]
Co_3O_4 nanoparticle decorated ultrathin porous nanosheets	0.01-3.0	0.18 A g^{-1}	888.8 (80)	22.2 (4.5 A g^{-1})	[16]
SnO_2@Co_3O_4 hollow nanospheres	0.01-2.5	0.1 A g^{-1}	982 (100)	750 (0.9 A g^{-1})	[17]
Hollow SnO_2@Co_3O_4 core shell spheres	0.05-3.0	0.2 A g^{-1}	815 (100)	380 (1.0 A g^{-1})	[18]

SnO_2-Co_3O_4 core-shell nanoneedle arrays	0.001-3.0	0.5 A g^{-1}	985 (100)	219 (12.0 A g^{-1})	[19]
Janus-structured mutually doped hollow SnO_2-Co_3O_4	**0.001-3.0**	**1 .0 A g^{-1}**	**1058.7 (1000)**	**666.3 (10.0 A g^{-1})**	**Our work**

References

[1] V. Etacheri, G. A. Seisenbaeva, J. Caruthers, G. Daniel, J.-M. Nedelec, V. G. Kessler, V. G. Pol, *Adv. Energy Mater.*, 2015, **5**, 1401289.

[2] G. D. Park, J,-K. Lee, Y. C. Kang, *Adv. Funct. Mater.*, 2017, **27**, 1603399.

[3] G. D. Park, Y. C. Kang, *Nano Res.*, 2017, DOI 10.1007/s12274-017-1744-7.

[4] X. Liu, J. Zhang, W. Si, L. Xi, S. Oswald, C. Yan, O. G. Schmidt, *Nanoscale*, 2015, **7**, 282-288.

[5] H. Kim, J. Cho, *J. Mater. Chem*, 2008, **18**, 771-775.

[6] X. M. Yin, C. C. Li, M. Zhang, Q. Y. Hao, S. Liu, L. B. Chen, T. H. Wang, *J. Phys. Chem. C*, 2010, *114*, 8084-8088.

[7] J. S. Cho, H. S. Ju, Y. C. Kang, *Sci. Rep.*, 2016, **6**, 23915.

[8] T. Yang, B. Lu, *Phys. Chem. Chem. Phys.*, 2014, **16**, 4115-4121.

[9] Y. Li, B. Tan, Y. Wu, *Nano Lett.*, 2008, **8**, 265-270.

[10] X. Wang, X.-L. Wu, Y.-G. Guo, Y. Zhong, X. Cao, Y. Ma, J. Yao, *Adv. Funct. Mater*., 2010, **20**, 1680-1686.

[11] D. Wang, Y. Yu, H. He, J. Wang, W. Zhou, H. D. Abruna, *ACS Nano*, 2015, **9**, 1775-1781.

[12] G. Huang, S. Xu,S. Lu, L. Li, H. Sun, *ACS Appl. Mater. Interfaces*, 2014, **6**, 7236-7243.

[13] S. Chen, Y. Zhao, B. Sun, Z. Ao, X. Xie, Y. Wei, G. Wang, *ACS Appl. Mater. Interfaces*, 2015, **7**, 3306-3313.

[14] H. Huang, W. Zhu, X. Tao, Y. Xia, Z. Yu, J. Fang, Y. Gan, W. Zhang, *ACS Appl. Mater. Interfaces.*, 2012, **4**, 5974-5980.

[15] N. Yan, L. Hu, Y. Li, Y. Wang, H. Zhong, X. Hu, X. Kong, Q. Chen, *J. Phys. Chem. C*, 2012, **116**, 7227-7235.

[16] J. Mujtaba, H. Sun, G. Huang, K. Mølhave, Y. Liu, Y. Zhao, X. Wang, S. Xu, J. Zhu, *Sci. Rep*., 2016, **6**, 20592.

[17] W. S. Kim, Y. Hwa, H.-C. Kim, J.-H. Choi, H.-J. Sohn, S.-H. Hong, *Nano Res.*, 2014, **8**, 1128–1136.

[18] B. Zhao, S.-Y. Huang, T. Wang, K. Zhang, M. M. F. Yuen, J.-B. Xu, X.-Z. Fu, R. Sun, C.-P. Wong, *J. Power Sources*, 2015, **298**, 83-91.

[19] L.-L. Xing, Y.-Y. Zhao, J. Zhao, Y.-X. Nie, P. Deng, Q. Wang, X.-Y. Xue, *J. Alloys Compd.*, 2014, **586**, 28-33.